

Validation of MARS-KS models for the Passive Containment Cooling System of i-SMR and Application to Containment Transient Analysis

Changyong Jung ^a, Hyeonjo Kim ^a, Yeon-Gun Lee ^{a*}

^aDepartment of Quantum and Nuclear Engineering, Sejong University
209, Neungdong-ro, Gwangjin-gu, Seoul, Republic of Korea

*Corresponding author: yglee@sejong.ac.kr

***Keywords :** Innovative Small Modular Reactor(i-SMR), Passive Containment Cooling System(PCCS), MARS-KS code, Condensation

1. Introduction

In the Korean innovative small modular reactor (i-SMR) under development, the Passive Containment Cooling System (PCCS) mitigates design-basis accidents by condensing steam on the outer surfaces of vertical heat-exchanger tubes and rejecting heat to the Emergency Cooling Tank (ECT) via a density-driven natural-circulation loop. PCCS condensation in the i-SMR is characterized by (1) *Near-vacuum Containment Vessel (CV) during normal operation, leading to negligible non-condensable gas content and a steam-dominated atmosphere at accident initiation;* (2) *Condensation on the outer surface of vertically oriented heat exchanger tubes;* (3) *Relatively high accident pressures in the CV, up to 40 bar, compared with large nuclear power plants;*

Under these conditions, CV depressurization and long-term heat removal become highly sensitive to phase-change heat transfer and condensate drainage, while boiling inside the passive heat exchanger may induce natural-circulation flow instabilities that can impair PCCS heat-removal performance. Therefore, this study assesses whether the safety analysis code MARS-KS can reliably predict the phase-change heat transfer governing PCCS performance.

2. Phase change heat transfer Model in MARS-KS code

In the default condensation heat transfer model embedded in MARS-KS code, the heat transfer coefficient for pure steam condensation is estimated when the mass fraction of non-condensable gas is smaller than 10^{-9} . Under this condition, the larger heat-transfer coefficient between the Nusselt correlation [1] and the Shah correlation [2] is used. When non-condensable gases are present, the Colburn–Hougen model [3] is employed. In this approach, the heat fluxes through the liquid film and the diffusion layer are iteratively calculated until their balances are achieved to determine the converged heat transfer coefficient [4].

Table I: Condensation model implemented in MARS-KS code

Nusselt correlation	$h = 0.943 \left[\frac{k_i^3 \rho_i^2 h_{fg}}{\mu_i (T_{sat} - T_w) L} \right]^{1/4}$ (1)
Shah correlation	$h_{TP} = h_L \left[(1-x)^{0.8} + \frac{3.8x^{0.76}(1-x)^{0.04}}{Pr^{0.38}} \right]$ (2)
	$h_c = \max(h_{Nu}, h_{Sh})$ (3)
	$q_i'' = h_c (T_{vi} - T_w)$ (4)
Colburn-Hougen	$q_v'' = h_m h_{fgb} \frac{\rho_{vb}}{x_{vb}} \ln \left(\frac{1 - \frac{p_{vi}}{p}}{1 - \frac{p_{vb}}{p}} \right)$ (5)

MARS-KS code models in-tube boiling through a regime-dependent wall heat-transfer. Nucleate boiling is typically treated using a Chen-type correlation, while Critical Heat Flux (CHF) is predicted using CHF lookup tables, followed by post-CHF/film-boiling heat transfer modeling [4].

3. Validation against condensation separate effects tests

The condensation separate-effects tests (SET) selected in this study were conducted at Seoul National University (SNU) [5], Harbin Engineering University (HEU) [6], and KAIST [7,8]. All three experiments measured the condensation heat transfer coefficient using a vertical tube; however, each dataset has limitations with respect to the expected containment conditions of the Korean i-SMR PCCS. In the SNU and HEU tests, a relatively high fraction of non-condensable gas was present, and the maximum test pressure was

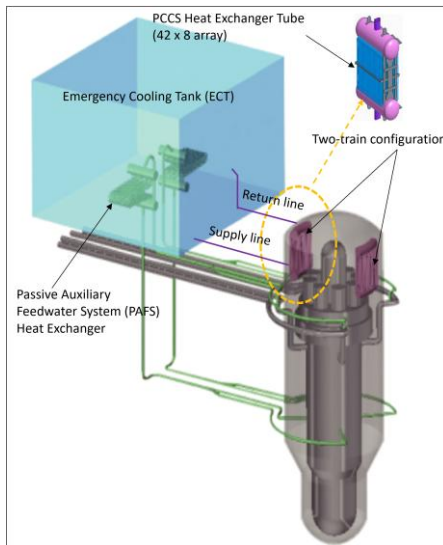


Fig.1. Component of i-SMR PCCS

lower than the peak pressure anticipated in the i-SMR containment. The KAIST test provides high-pressure condensation data for pure steam up to 7.5 MPa, but it represents condensation on the inner wall of a vertical tube, resulting in a condensing geometry that differs from that of the PCCS heat exchanger.

Consequently, no single experiment currently available fully captures the accident relevant atmospheric conditions in the CV and the geometry of the condensing surface. Therefore, using the above SET datasets among which the vertical-tube tests provide comparatively higher-pressure conditions constitute the most practical and effective validation strategy at this stage.

3.1 MARS-KS validation with SNU and HEU condensation SETs

For the SNU and HEU test simulations, the test vessel was nodalized into six control volumes forming a natural-circulation loop. Condensation was modeled by applying heat structures only to the upper downflow volumes with the measured wall temperature imposed as the boundary condition.

The secondary-side coolant in the heat-exchanger tube was not modeled; instead, the experimentally measured wall temperature was prescribed as a boundary condition for the heat structure. MARS-KS code does not allow the wall temperature to be specified directly at the fluid-structure interface, the prescribed temperature was applied at the opposite side of the heat structure. The heat transfer coefficient was then evaluated as

$$h = q'' / \Delta T_{sub} \quad (6)$$

where q'' is the wall heat flux and ΔT_{sub} is the wall subcooling

Because both experiments were performed under natural-convection conditions, an outlet pressure boundary condition was not imposed, as prescribing such a condition could artificially generate forced convection and consequently alter the intrinsic flow behavior of the system. Instead, steam was supplied through a time-dependent inlet boundary, and the system pressure was maintained at a constant value during steam injection using a control variable that compensated for pressure reduction resulting from steam condensation.

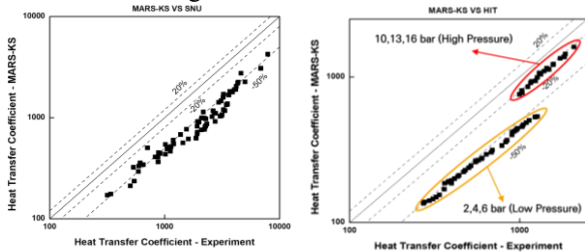


Fig.2. Comparison of heat transfer coefficient: MARS-KS vs SNU experiment

Fig.3. Comparison of heat transfer coefficient: MARS-KS vs. HEU experiment

The mean relative errors between the experimental data (SNU and HEU) and the MARS-KS code predictions exceeded 50% for both SETs, indicating a generally low level of predictive accuracy.

3.2 MARS-KS validation with KAIST condensation SET

Whereas Section 3.1 validated MARS-KS code against condensation data measured on the outer surface of a vertical tube under steam-air natural-convection conditions, this section examines the KAIST tests, which provide high-pressure condensation data under pure-steam condition. The region of interest was discretized into ten axial control volumes. The upper section was modeled as adiabatic, and condensation heat transfer was applied only to the remaining segments.

The pressure condition was controlled through an outlet TMDPVOL. The steam mass flow rate was adjusted using a TMDPJUN according to the experimental conditions. Because the first node of the test section of interest was insulated in the experiment, the heat structure was connected only to nine of the ten fluid nodes. The boundary conditions for the heat structure were imposed in the same manner as SNU, HEU simulations.

Fig.4 and 5 present the validation results based on the condensation test conducted at KAIST. With an emphasis on the validation at high pressure, test runs conducted at 4.559 MPa and 6.656 MPa were selected. The axial distributions of the local heat transfer coefficient and the condensate mass flow rate were compared with predictions from RELAP5-3D [7], NRELAP5 [7], and MARS-KS.

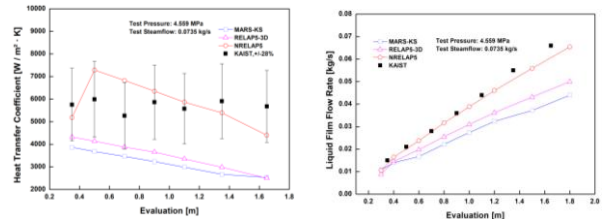


Fig.4. Validation result at pressure = 4.559 MPa, mass flow rate = 0.0735kg/s

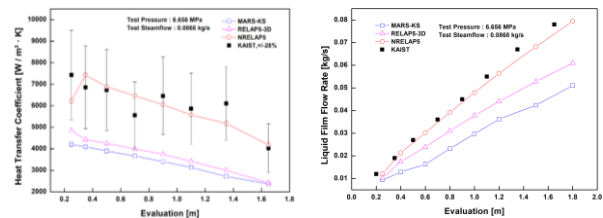


Fig.5. Validation result at pressure = 6.656 MPa, mass flow rate = 0.0868kg/s

The results show that MARS-KS underpredicts the heat transfer coefficient over the entire axial range compared to the experimental data and consequently predicts a lower condensate mass flow rate.

From a containment integrity perspective, underpredicting the condensation heat-transfer

coefficient leads to an underestimation of the PCCS heat removal by condensation, thereby increasing the predicted mass and energy retention in the containment. As a result, the containment pressure and temperature are predicted to be higher than they would be with more accurate condensation modeling.

From a LOCA performance perspective, because i-SMR designs cool the core by recirculating condensate during a LOCA, underpredicting the condensation rate delays coolant accumulation in the lower containment. This, in turn, yields lower predicted recirculation flow and core liquid inventory and a higher predicted Peak Cladding Temperature (PCT). Overall, both the containment integrity assessment and the LOCA performance evaluation become conservative when condensation is underpredicted.

4. Validation of in-tube flow instability

Flow oscillations can degrade the heat removal performance of the PCCS and may induce mechanical fatigue of system structures. Therefore, during normal operation and under DBA conditions, it is necessary to demonstrate that flow instabilities do not occur in the PCCS, and the safety analysis code needs to appropriately predict such phenomena.

To evaluate the predictive capability of MARS-KS for flashing-induced flow instabilities, the CIRCUS facility conducted at Delft University of Technology [9], which simulates natural-circulation flashing under low-pressure conditions, was selected as an in-tube flow-instability validation experiment.

In the TU Delft experiment simulation, detailed information on the secondary side was not available. Therefore, the inlet temperature was controlled to be close to the experimental value by adjusting the heat exchanger and the buffer tank. In addition, to reproduce a thermal equilibrium condition at steady state, the heat production rate 8000 W was applied to the core and same cooling rate was applied to the heat exchanger.

The buffer tank mitigates fluctuations in the core inlet temperature and pressure due to its large volume. Furthermore, the heat structure was connected to the lowest of the four control volumes.

Table II: Validation results for the Delft experiment average period of flow oscillation by case [s]

Case \ Method	M06 Inlet temp 85.5 °C	M07 Inlet temp 87.3 °C	M08 Inlet temp 90.4 °C
Exp	80.6	68.0	48.8
RELAP5	78.2	67.3	49.5
MARS-KS	81.0	66.8	52.4

The mean period of the flow oscillations was compared with the experimental data. As shown in Table II, as the core inlet temperature increases, the region in

which single-phase flow is maintained decreases, and the period of the flow oscillation correspondingly decreases.

The mean absolute percentage error (MAPE) of the predicted quantity was 0.46%, 1.84%, and 7.38% for cases M06, M07, and M08, respectively. This indicates reasonable agreement for M06 and M07 (errors below 2%). Although the error tends to increase as the wall subcooling decreases, as observed in case M08, the difference is modest (approximately 7%) and can be regarded as minor.

5. MARS-KS input model for preliminary analysis of the i-SMR PCCS

For a preliminary evaluation of PCCS cooling performance, a simplified MARS-KS model consisting only of the CV and the PCCS was developed, and the resulting containment pressure and temperature transients were analyzed

In the present input model, an inadvertent EDV opening accident was assumed. The containment vessel and PCCS nodalization were established as illustrated in fig.6, reflecting the PCCS design specifications.

In this model, the 168 tubes comprising each heat exchanger bundle were integrated into a single PIPE component. The CV atmosphere was initialized under vacuum conditions. The containment heat structures were connected to the internal control volume of the containment, and the opposite boundary was specified to represent heat losses to the external environment by imposing an ambient temperature of 333.15 K and an external convective heat-transfer coefficient of 5 W/m²·K.

In an actual i-SMR, the steam discharge rate to the steel containment during an inadvertent EDV opening depends on the containment pressure. However, the present model does not include the reactor primary system, thus the released coolant mass and energy were prescribed as fixed boundary conditions. Accordingly, the present analysis focuses on the containment pressure response under these specified release conditions. Steam injection to simulate coolant release was modeled by defining TMDPVOL as the source component and connecting it to the system through TMPDJUN. Fig 7 shows the released steam mass flow rate.

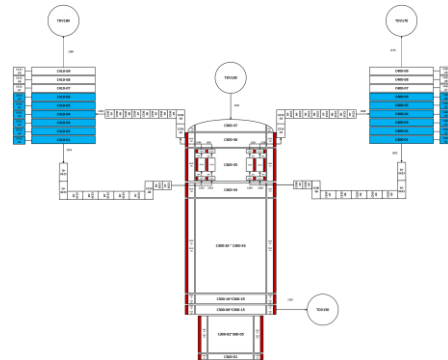


Fig. 6. Nodalization of i-SMR CV and PCCS for preliminary analysis of containment response.

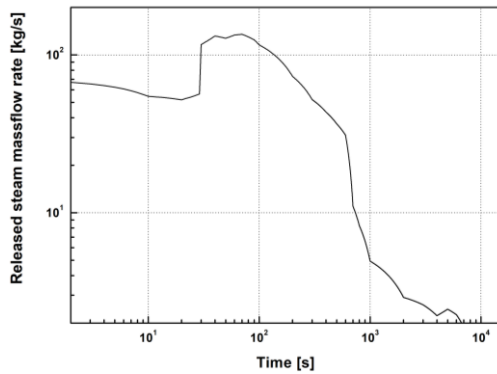


Fig. 7. Released steam mass flow rate.

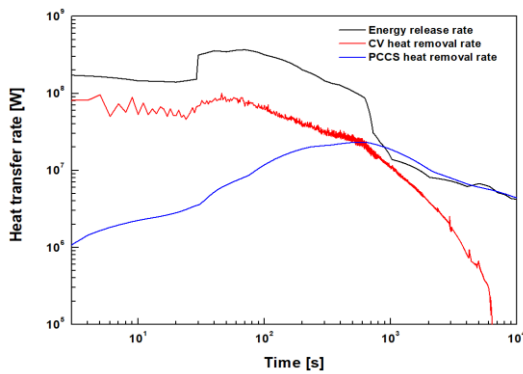


Fig. 8. Heat removal rate of PCCS and CV

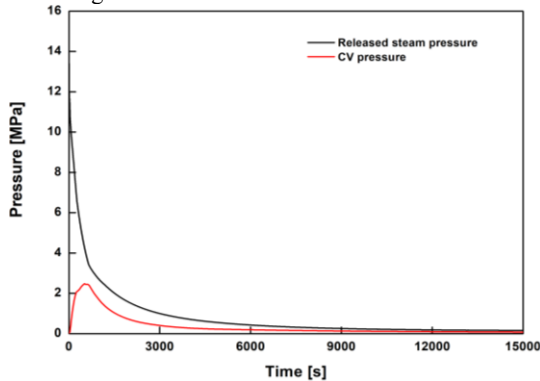


Fig. 9. Pressure transients of the CV and released steam

As shown in Fig. 8, during the initial transient phase, the injected energy is removed primarily through heat transfer to the containment wall. From approximately 800 s after the accident, the PCCS heat removal rate exceeds the heat transfer rate to the containment wall.

After about 10 minutes, the total heat removal rate by the PCCS and the containment wall becomes greater than the total energy release rate, and the containment pressure and temperature begin to decrease. In a typical LOCA scenario, the Emergency Recirculation Valve (ERV) opens immediately, leading to a rapid pressure increase in the CV due to the flashing of the primary coolant and the sudden inflow of mass and energy. However, the primary system was not explicitly modeled in this analysis, and the ERV was not included in the nodalization. Instead, a control variable was implemented to maintain a constant water level in the CV,

when the condensate level exceeds 5.34 m, the excess water is artificially drained to TMDPVOL. The initial coolant discharge through the ERV during the early accident phase was not adequately reflected in the simulation, which restricted the initial surge of mass and energy into the CV. Therefore, the insufficient representation of the early ERV-mediated coolant release is considered the primary reason for the relatively low peak pressure (~ 2.5 MPa) predicted in our results compared with other studies that predicted the CV pressure could reach 4.0 MPa [10].

Although the preliminary analysis indicates that the MARS-KS code underestimates the condensation heat-transfer coefficient, Fig. 9 confirms that the containment pressure decreases to below 50% of the peak pressure within 24 hours.

6. Conclusions

To evaluate the applicability of the condensation heat-transfer model implemented in the regulatory safety analysis code MARS-KS for PCCS applications, validation was performed against condensation separate-effects test data from SNU, HEU, and KAIST. The comparison results indicate that MARS-KS may underpredict the condensation heat-transfer coefficient by up to 50% under high-pressure conditions. Because the vertical-tube experimental database employed in this study does not include pure-steam condensation data at high pressure, future work should prioritize establishing an i-SMR-representative integral thermal-hydraulic experimental database, followed by additional validation and potential model improvements.

For future i-SMR analyses, further investigations will be conducted to quantify modeling uncertainties associated with

(i) Representing the PCCS heat exchanger tube bundle by integrating multiple tubes into a single equivalent channel versus explicitly modeling the tube bundle with multiple channels.

(ii) Modeling the containment volume using a one-dimensional representation versus a three-dimensional representation leveraging the Multi-D capability of MARS-KS. The impact of these modeling choices on predicted containment pressure transient behavior during accident conditions will be systematically assessed.

ACKNOWLEDGEMENTS

This work was supported by the Nuclear Safety Research Program through the Regulatory Research Management Agency for SMRs (RMAS) and the Nuclear Safety and Security Commission (NSSC) of the Republic of Korea. (No. RS-2024-00509653) and by the National Research Foundation of Korea grant funded by the Korean Government (MSIT) (No. RS-2025-02353161)

REFERENCES

- [1] Nusselt, W. Die Oberflächenkondensation des Wasserdampfes. Zeitschrift des Vereins Deutscher Ingenieure, 60, 541–546, 569–575, 1916.
- [2] Shah, M. M. A general correlation for heat transfer during film condensation inside pipes. International Journal of Heat and Mass Transfer, 22(4), 547–556, 1979.
- [3] Colburn, A. P., & Hougen, O. A. Design of cooler condensers for mixtures of vapors with non-condensable gases. Industrial & Engineering Chemistry, 26(11), 1178–1182, 1934.
- [4] MARS code manual: Volume V, Models and correlations (KAERI/TR-3872/2009). Korea Atomic Energy Research Institute, Daejeon, Republic of Korea.
- [5] Kim, J.-W., Lee, Y.-G., Ahn, H.-K., Park, G.-C. Condensation heat transfer characteristic in the presence of non-condensable gas on natural convection at high pressure. Nuclear Engineering and Design, 239(4), 688-698, 2009.
- [6] Bian, H., Lu, Y., Li, C., Liang, T., and Ding, M. Comprehensive parameter analyses on steam-air condensation at pressures up to 1.6 MPa. Nuclear Engineering and Design 385, 115136, 2021.
- [7] Kim, S. J. Turbulent film condensation of high pressure steam in a vertical tube of passive secondary condensation system (Doctoral dissertation, Korea Advanced Institute of Science and Technology, Daejeon, Republic of Korea), 2000.
- [8] Sawant, P., Marking, J., & Delfino, C. NRELAP5 predictions of KAIST high pressure condensation data using existing and extended Shah condensation correlation. Proceedings of NURETH-16: The 16th International Topical Meeting on Nuclear Reactor Thermal Hydraulics (Chicago, IL, USA, Aug. 30–Sept. 4, 2015).
- [9] Annalisa Manera & Tim H. J. J. van der Hagen Stability of Natural - Circulation-Cooled Boiling Water Reactors during Startup: Experimental Results, Nuclear Technology, 143:1, 77-88, 2003.
- [10] Yoon, S. (2026, March 20). Current status and issues of innovative SMR technology development [Lecture slides]. SMR System Design Group, SMR Development Research Institute, KHNP Central Research Institute.